The EMBO Journal vol.14 no.12 pp.2731–2744, 1995

Targeting of *Listeria monocytogenes* ActA protein to the plasma membrane as a tool to dissect both actin-based cell morphogenesis and ActA function

Evelyne Friederich[1], Edith Gouin[2], Raymond Hellio[1], Christine Kocks[2,3], Pascale Cossart[2] and Daniel Louvard[1,4]

[1]Institut Pasteur, Unité de Biologie des Membranes, CNRS, UMR 144, 25 rue du Docteur Roux and [2]Institut Pasteur, Unité des Interactions Bactéries-Cellules, CNRS URA 1300, 28 rue du Docteur Roux, 75724 Paris Cedex 15, France
[3]Present address: Institut für Genetik, Universität zu Köln, Zülpicher strasse 47, 50674 Köln, Germany

[4]Corresponding author

Actin assembly on the surface of *Listeria monocytogenes* in the cytoplasm of infected cells provides a model to study actin-based motility and changes in cell shape. We have shown previously that the ActA protein, exposed on the bacterial surface, is required for polarized nucleation of actin filaments. To investigate whether plasma membrane-associated ActA can control the organization of microfilaments and cell shape, variants of ActA, in which the bacterial membrane signal had been replaced by a plasma membrane anchor sequence, were produced in mammalian cells. While both cytoplasmic and membrane-bound forms of ActA increased the F-actin content, only membrane-associated ActA caused the formation of plasma membrane extensions. This finding suggests that ActA acts as an actin filament nucleator and shows that permanent association with the inner face of the plasma membrane is required for changes in cell shape. Based on the observation that the amino-terminal segment of ActA and the remaining portion which includes the proline-rich repeats cause distinct phenotypic modifications in transfected cells, we propose a model in which two functional domains of ActA cooperate in the nucleation and dynamic turnover of actin filaments. The present approach is a new model system to dissect the mechanism of action of ActA and to further investigate interactions of the plasma membrane and the actin cytoskeleton during dynamic changes of cell shape.

Key words: ActA/actin nucleation/CAAX box/motility/transfection

Introduction

Interaction between the plasma membrane and the underlying cortical cytoskeleton plays an important role in cellular functions such as cell motility and morphogenesis. Spatially controlled nucleation of actin filaments at the plasma membrane interface, and the establishment of physical linkages between actin filaments and the plasma membrane, are crucial for the assembly of F-actin structures involved in these processes (Small *et al.*, 1978; Hartwig and Shelvin, 1986; Okabe and Hirokawa, 1989; Cunningham *et al.*, 1992). Moreover, it has been proposed that rapid turnover of these membrane-associated actin filaments is one of the driving forces for plasma membrane protrusion (Wang, 1985; Forscher and Smith, 1988; Theriot and Mitchison, 1991; Forscher *et al.*, 1992). Because it is difficult to dissect plasma membrane actin cytoskeleton interactions at the molecular level, little is known about the factors participating in the nucleation of actin filaments and in their association with the plasma membrane. Ponticulin, the only integral membrane protein reported to nucleate actin filaments, has so far only been detected in lower eukaryotes (Wuestehube and Luna, 1987; Shariff and Luna, 1990; Hitt *et al.*, 1994a,b). However, since direct binding of actin to the inner surface of stripped plasma membranes has been observed in higher eukaryotes, proteins with properties similar to those of ponticulin might exist in these cells (Hubbard and Ma, 1983; Tranter *et al.*, 1989).

The properties of the bacterial pathogen *Listeria monocytogenes* provide a new model system to study the assembly of F-actin structures and actin-based membrane dynamics in higher eukaryotic cells. After invasion of the host cytoplasm, the bacterium uses the host actin cytoskeleton for intracellular movement and to spread from cell to cell. The bacterium forms a tail-like F-actin structure to which intracellular actin-associated proteins are recruited (Tilney and Portnoy, 1989; Dabiri *et al.*, 1990; Tilney *et al.*, 1990, 1992a,b; Dold *et al.*, 1994; Temm-Grove *et al.*, 1994; Theriot *et al.*, 1994; for reviews see Cossart and Kocks, 1994; Cossart, 1995). The tail structure, the formation of which is required for intracytoplasmic movement and cell–cell spreading (Domann *et al.*, 1992; Kocks *et al.*, 1992), is composed of short, cross-linked actin filaments which rapidly turn over (Theriot *et al.*, 1992; Tilney *et al.*, 1992a). These processes are reminiscent of those involved in actin-based motility and morphogenesis, and opened the way to study actin filament assembly in the absence of the plasma membrane.

The polarized nucleation of actin filaments, which results in the formation of the tail structure at one extremity of the bacteria, is dependent on the expression of the bacterial *actA* gene (Domann *et al.*, 1992; Kocks *et al.*, 1992). This gene encodes a protein of 639 amino acid residues which is exposed on the bacterial surface in a polarized fashion (Kocks *et al.*, 1992, 1993). Transfection experiments with cultured eukaryotic cells indicated that ActA may act as an actin filament nucleator (Pistor *et al.*, 1994). In these experiments, ActA was targeted to the outer membrane of mitochondria and caused the accumulation of F-actin on the surface of these organelles (Pistor *et al.*, 1994). Since bacteria nucleate actin only poorly *in vitro*

(Tilney *et al.*, 1992b), it has been proposed that ActA may either bind cellular factors implicated in actin assembly or be modified *in vivo*. Several reports demonstrated the functional importance of the proline-rich repeats and proposed that they may mediate the association of ActA with cellular factors necessary for nucleation (Pistor *et al.*, 1994; Southwick and Purich, 1994; Theriot *et al.*, 1994). Profilin depletion experiments in *Xenopus* egg extracts which support actin-based movement of *L.monocytogenes* indicated that one of these factors may be profilin (Theriot *et al.*, 1994), a protein involved in the control of actin polymerization (for reviews see Machesky and Pollard,1993; Sohn and Goldschmidt-Clermont, 1994).

Since ActA is able to initiate a cascade of events leading to the formation of a specific F-actin structure and membrane protrusions which contain bacteria, it is tempting to speculate that actin assembly is normally under the control of an endogenous protein with properties similar to those of ActA. Previous studies indicated that nucleation of actin filaments occurs near the inner surface of the plasma membrane (Small *et al.*, 1978; Wang, 1985; Forscher and Smith, 1988; Okabe and Hirokawa, 1989; Theriot and Mitchison, 1991; Forscher *et al.*, 1992). Thus, an endogenous nucleator should be located at this site. However, the activity of ActA has so far only been investigated in the cytoplasm in transfected cells (Pistor *et al.*, 1994). To obtain further information on the mechanism of action of ActA and on the role of plasma membrane-associated actin assembly in cellular morphogenesis, we engineered an ActA variant which is stably associated with the inner face of the plasma membrane by the plasma membrane localization signal of K-ras (Hancock *et al.*, 1990, 1991). Transient transfection of DNA constructs encoding genetically engineered ActA variants into cultured cells was used to study the effects of these variants on the organization of the actin cytoskeleton and on cell shape. The effects of the plasma membrane-associated ActA variant and of a cytoplasmic form of ActA were compared in transfected cells. Our results demonstrate that ActA causes different effects on the organization of the actin cytoskeleton and cell shape, depending on the intracellular compartment to which it is targeted. Furthermore, we show that the changes caused by the membrane-associated ActA variant are a sensitive functional assay for the activity of ActA deletion variants. Our results provide the first direct evidence that ActA is composed of at least two functional domains which exert distinct effects on the organization of the actin cytoskeleton in transfected cells.

Results

Description of recombinant DNAs encoding ActA variants and ActA–K-ras (B) hybrid proteins

We constructed two ActA variants to compare the consequences of ActA production in the cytoplasm or on the inner face of the plasma membrane. The first construct (for cytoplasmic localization), ActA(1–584), corresponds to the portion of the ActA sequence which is exposed on the bacterial surface (Figure 1A). This variant lacked the putative membrane anchor domain previously shown to target ActA to the outer membrane of mitochondria in *actA*-transfected cells (Pistor *et al.*, 1994). Moreover, to prevent insertion into the endoplasmic reticulum, the signal peptide was removed and a eukaryotic translation start site was introduced. In the second ActA variant, ActA(1–584)–CAAX, the hydrophobic C-terminal anchor was replaced by the plasma membrane localization signal of K-ras (B). It has been shown previously, that this 17 amino acid long sequence is sufficient to localize heterologous proteins to the inner surface of the plasma membrane (Hancock *et al.*, 1991; Leevers *et al.*, 1994; Stokoe *et al.*, 1994). The sequence comprises a CAAX motif which is post-translationally modified (farnesylation at the cysteine residue, proteolytic cleavage of the AAX amino acids and methylesterification at the C-terminal cysteine) and a polybasic domain, both of which are required for stable plasma membrane association of K-ras (B) (Hancock *et al.*, 1990, 1991). We predicted that ActA should be inserted via this sequence into the inner leaflet of the plasma membrane and exposed to the cytosol, as it is when present on the bacterial surface. In order to determine the functionally important segments of ActA, four shorter constructs were engineered, ActA(235–584)–CAAX and ActA(1–234)–CAAX, both of which were fused to the K-ras sequence, as well as ActA(235–584) and ActA(1–234), which were lacking this sequence. For expression in eukaryotic cells, the recombinant DNAs were inserted into the pCB6 expression vector, in which expression of inserted DNAs is under the control of the cytomegalovirus promotor.

Production of ActA variants in transfected cells

In order to verify the production of the ActA variants, lysates of transiently transfected HeLa cells were analysed by immunoblotting using antibodies directed against a 22 amino acid long synthetic peptide which comprises the first part of one of the proline-rich repeats of ActA (Kocks *et al.*, 1993). Analysis of cells transfected with DNAs encoding ActA(1–584) or ActA(1–584)–CAAX revealed protein bands which specifically reacted with anti-ActA antibodies and migrated at positions corresponding to apparent M_rs of 87 and 92 kDa, respectively (Figure 1B, lanes 2 and 3). Minor higher M_r forms of these ActA variants could frequently be observed. These proteins were not detected in untransfected cells (lane 1). The apparent M_r of these ActA variants was higher than that expected from the protein primary sequence and was close to that observed for the ActA protein synthesized by *L.monocytogenes* (Kocks *et al.*, 1992). ActA(1–234)–CAAX, which was detected with an antipeptide antibody specific for an amino-proximal sequence of ActA, exhibited an apparent M_r of 42 kDa and migrated as a single band (lane 6). In contrast, ActA(235–584)–CAAX, which contains the entire proline-rich repeat region, migrated as a quadruplet or a triplet of 56–71 kDa (Figure 1B, lane 4). Since it was previously demonstrated that intracellular wild-type ActA is phosphorylated (Brundage *et al.*, 1993), we determined whether this was also the case for ActA(235–584)–CAAX. The cell lysate was treated with calf intestinal alkaline phosphatase (Figure 1C). Compared with the control sample which was incubated in the absence of enzyme (Figure 1C, lane 1), phosphatase treatment shifted the higher molecular form to the lower one (Figure 1C, lane 2). This result strongly suggests that the ActA(235–584)–CAAX variant is phosporylated.

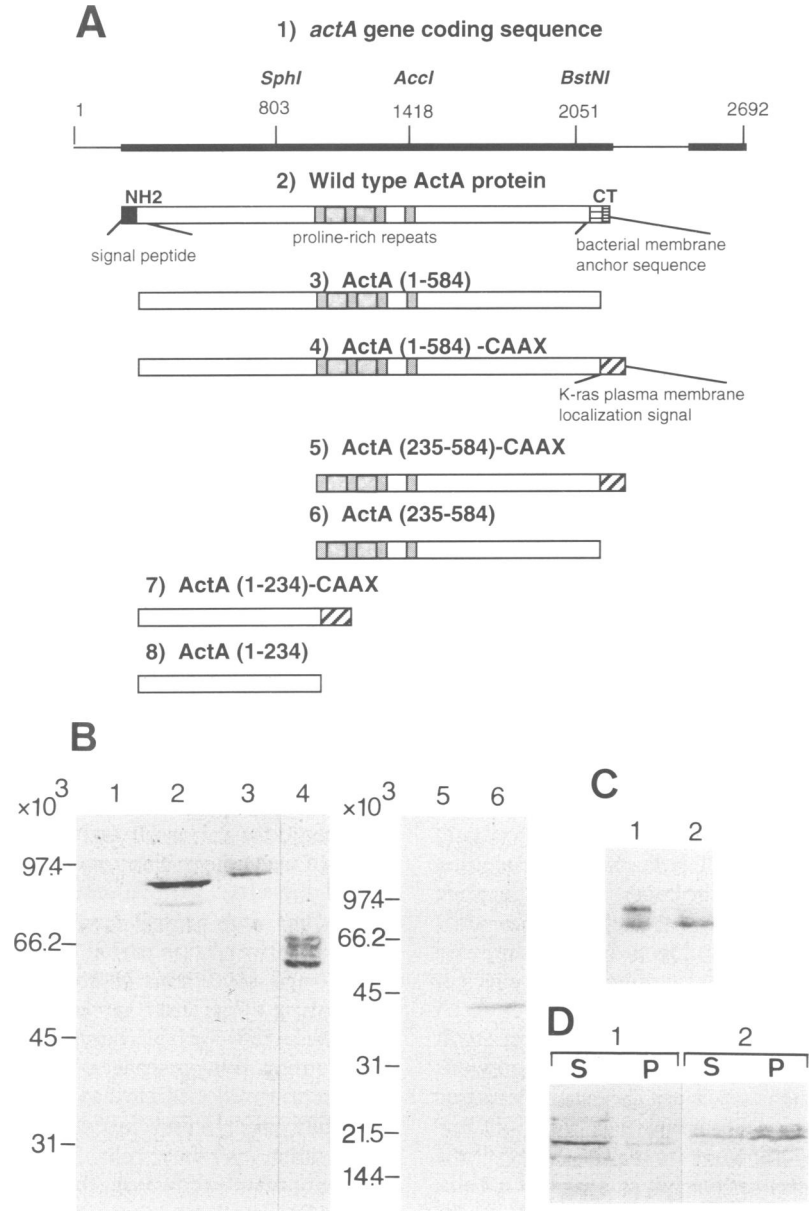

Fig. 1. Production of ActA variants and ActA–CAAX hybrid proteins in transiently transfected HeLa cells. (**A**) Construction of ActA variants and K-ras hybrid proteins. (1) The *actA* gene coding sequence, corresponding to residues 1–2692 of the *L.monocytogenes* lecithinase operon, is represented by the thick line. Thin lines correspond to untranslated sequences. Restriction sites used to engineer the constructs are indicated. Procedures used to generate the constructs are described in detail in Materials and methods. All *actA* DNA constructs were inserted into the eukaryotic cytomegalovirus-derived pCB6 expression vector. (2–8) Schematic representation of the primary structures of wild-type ActA, ActA deletion and K-ras hybrid proteins. (2) Organization of the primary structure of the wild-type ActA protein. (3) Deletion of the *actA* gene sequences encoding the putative signal peptide and the bacterial membrane anchor sequence yielded ActA(1–584) containing amino acids 1–584 of the native ActA primary sequence. (4) In-frame fusion of a sequence encoding the plasma membrane localization signal of K-ras (CAAX) to the 3′ end of the DNA construct encoding ActA(1–584) yielded ActA(1–584)–CAAX. The four shorter ActA variants, (5) ActA(235–584)–CAAX, (6) ActA(235–584), (7) ActA(1–234)–CAAX and (8) ActA(1–234) included amino acids 235–584 (5 and 6) and 1–234 (7 and 8) of the ActA primary sequence. Constructs (5) ActA(235–584)–CAAX and (7) ActA(1–234)–CAAX were both fused to the K-ras sequence. (**B**) Immunoblotting analysis of ActA variants in transfected HeLa cells. The transient production of ActA variants in HeLa cells transfected with the corresponding DNA constructs was analysed 48 h after transfection. Proteins in equivalent aliquots of cell lysates were separated on a 10% polyacrylamide–SDS gel under reducing conditions and transferred onto nitrocellulose membrane. Lane 1 (untransfected control cells), lane 2 [ActA(1–584)], lane 3 [ActA(1–584)–CAAX] and lane 4 [ActA(235–584)–CAAX] were incubated with affinity-purified polyclonal antibodies directed against a peptide corresponding to the proline-rich repeat of ActA. Lane 5 (untransfected cells) and lane 6 [ActA(1–234)–CAAX] were reacted with affinity-purified polyclonal antibodies specific for a sequence located near the amino-terminus of ActA. Molecular mass markers are indicated in kDa. (**C**) Phosphatase treatment of lysates of cells producing ActA(235–584)–CAAX. Lysates of HeLa cells transfected as described above with the DNA construct encoding ActA(235–584)–CAAX were incubated for 2 h in the absence (lane 1) or presence (lane 2) of calf intestinal phosphatase at 37°C. After phospatase treatment, samples were analysed by immunoblotting as described in B. (**D**) Immunoblotting analysis of fractions of HeLa cells producing ActA(1–584) or ActA(1–584)–CAAX. HeLa cells transfected as described in B were fractionated into 100 000 *g* cytosolic and crude membrane fractions. Equal volumes of the fractions were analysed by immunoblotting as described in B. D1: ActA(1–584), S: supernatant, P: pellet; D2: ActA(1–584)–CAAX, S: supernatant, P: pellet.

The association of ActA(1–584)–CAAX with the plasma membrane was demonstrated by cell fractionation. Cells transfected with constructs encoding ActA(1–584) or ActA(1–584)–CAAX were lysed and fractionated into cytosolic and crude membrane fractions. The distribution of the ActA variants between the two fractions was determined by immunoblot analysis (Figure 1D). While most of ActA(1–584) was found in the cytosol (Figure 1D1, S), most of ActA(1–584)–CAAX was detected in the membrane fraction (Figure 1D2, P), suggesting that the addition of the K-ras sequence results in the expected association of ActA with the plasma membrane.

The cytoplasmic ActA(1–584) variant induces F-actin assembly in the cytoplasm of transfected cells

Recombinant DNAs encoding ActA variants were transiently transfected into two different cell lines, the fibroblast-like monkey kidney CV-1 cells and the non-polarized epithelial human carcinoma HeLa cell line. In contrast to CV-1 cells, HeLa cells have a less organized actin cytoskeleton and are less spread. The effects of ActA variants on the organization of the actin cytoskeleton and on the morphology of transfected cells were qualitatively analysed using fluorescence, light and confocal laser scanning microscopy. Most of the phenotypic changes caused by ActA variants occurred in both cell lines but to different degrees.

To assess the effects of ActA located in the cytoplasm, cells were transfected with the DNA construct encoding ActA(1–584), which lacks both the bacterial signal peptide and membrane anchor sequence. After transfection, cells were stained with rhodamine-conjugated phalloidin, as a probe for F-actin, and by indirect immunofluorescence for ActA (Figure 2). The intracellular behaviour of this ActA variant was cell type dependent. In CV-1 cells, ActA was detected mainly in the nucleus, as reported in a previous study with PtK2 cells (Pistor *et al.*, 1994), and caused only a small increase in the intensity of cytoplasmic F-actin label (data not shown). In contrast, very little ActA(1–584) was detected in the nucleus of HeLa cells. Instead, most of the ActA label was located in the cytoplasm and was accompanied by a significant increase in the level of cytoplasmic F-actin compared with untransfected cells (Figure 2A, B). Interestingly, ActA stain co-distributed with that of F-actin in membrane protrusions (Figure 2A, B, arrowheads) where dynamic actin filament turnover occurs (Wang, 1985; DeBiasio *et al.*, 1988; Symons and Mitchison, 1991). However, despite the redistribution of F-actin, HeLa cells producing ActA(1–584) did not exhibit dramatic changes in cell shape and still formed asymmetric membrane protrusions, similar to those formed by untransfected cells.

The organization of the actin cytoskeleton in HeLa cells producing ActA(1–584) was further analysed by confocal laser scanning fluorescence microscopy. ActA(1–584)-positive cells were found to contain large amounts of F-actin label in the cell body, concomitant with the loss of stress fibres and the accumulation of ActA(1–584) and F-actin stainings in ruffled membranes (Figure 2D). A vertical section view of one such cell revealed that the F-actin label co-distributed with that of ActA throughout the whole cell body (Figure 2E, F). In contrast, F-actin staining in an ActA(1–584)-negative cell was limited to the cell cortex and was concentrated in specific F-actin-rich structures such as microvilli and stress fibres, as viewed in vertical section (see insert Figure 2F).

Plasma membrane-associated ActA causes the reorganization of the cortical actin cytoskeleton and changes in cell shape

Immunofluorescence analysis of HeLa cells producing ActA(1–584)–CAAX showed that the ActA label was homogeneously distributed all over the cell surface, a staining pattern typical of that of a plasma membrane-associated protein (Figure 3A). The F-actin staining co-distributed with that of ActA(1–584)–CAAX, and the cells did not exhibit prominent F-actin-containing structures such as stress fibres (Figure 3A, B). The same reorganization of the actin cytoskeleton was observed in CV-1 cells (data not shown). In contrast to the cytoplasmic ActA(1–584) variant, ActA(1–584)–CAAX induced both a redistribution of F-actin and important modifications of cell shape. These phenotypic modifications were particularly obvious in HeLa cells which are less well spread than CV-1 cells. While untransfected HeLa cells were spindle- or fan-shaped and formed polarized membrane protrusions, ActA(1–584)–CAAX-producing cells exhibited numerous lamellar membrane protrusions which frequently extended in a non-polarized manner (Figure 3A, B). Images showing a plane of focus at the ventral face of such cells revealed strong diffuse F-actin staining at the plasma membrane which was not observed in untransfected cells (Figure 3C, D and inserts). Vertical sections of the same cells revealed that the ActA(1–584)–CAAX label was restricted to the cell cortex and co-distributed with that of F-actin (Figure 3E, F and inserts). Interestingly, in contrast to untransfected cells (Figure 2F, insert) and cells producing the cytoplasmic ActA(1–584) variant (Figure 2E, F), these cells exhibited extremely thin peripheral membrane extensions and a reduction in dorsal surface protrusions such as microvilli (Figure 3E, F and inserts). It is noteworthy that the examination of these cells by phase contrast optics revealed an important reduction in membrane ruffles (data not shown). The formation of lamellar membrane extensions by ActA(1–584)–CAAX-positive cells was paralleled by an increase in their surface area. In contrast to untransfected cells and those producing ActA(1–584), these cells had, on average, a 20% larger cell surface ($n = 20$). While recruitment of F-actin to the plasma membrane was even observed in cells producing low amounts of ActA(1–584)–CAAX, modifications in cell shape only occurred when they produced high levels of the protein, as evaluated from the intensity of the immunofluorescence signal (Figure 6B). The rearrangement of the cortical actin cytoskeleton was accompanied by modification of cell–substratum interactions, as determined by interference reflection microscopy and immunostaining for vinculin as a marker for focal contacts. It is interesting to note that although they showed a strong reduction in well-organized focal adhesions, ActA(1–584)–CAAX-producing cells were well spread (data not shown). This phenotypic modification was particulary distinct in CV-1 cells, which form better organized focal contacts than HeLa cells.

The morphological changes observed with ActA(1–584)–CAAX were not due to non-specific effects caused

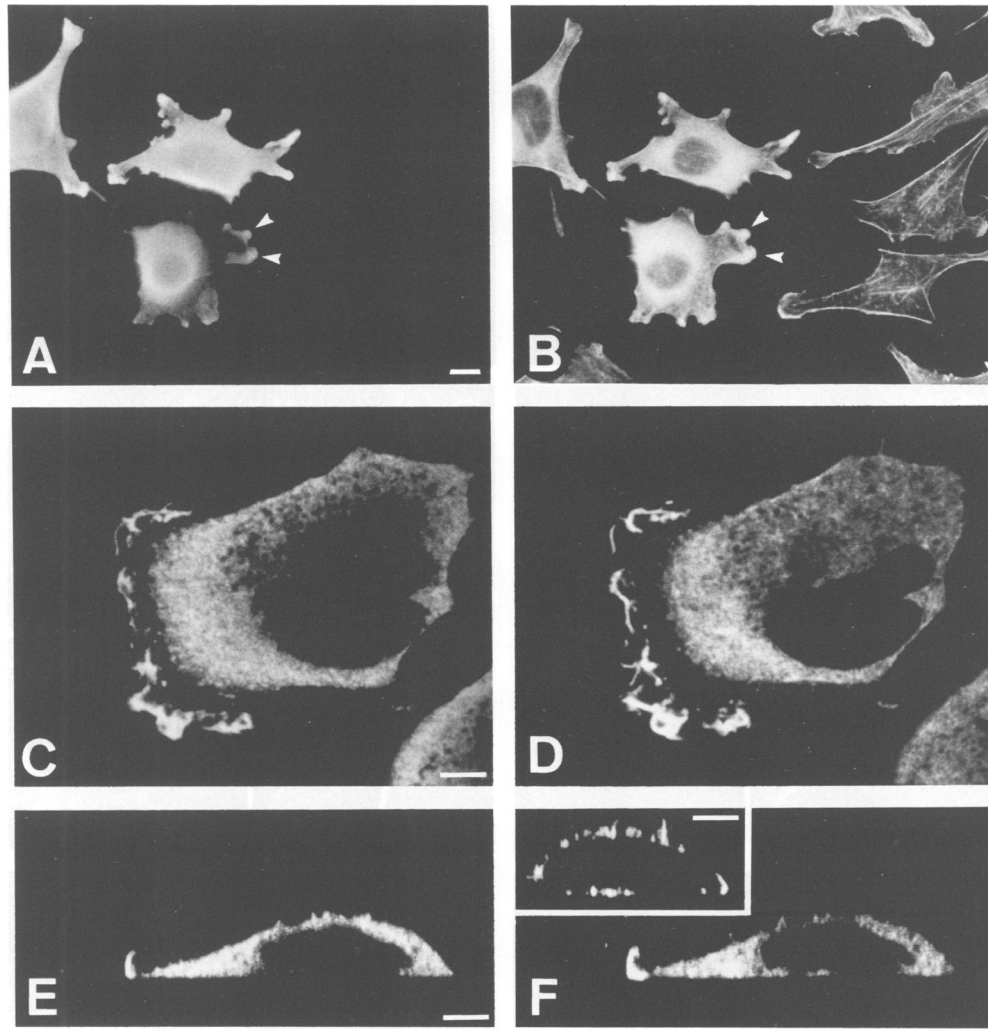

Fig. 2. Effects of cytoplasmic ActA(1–584) on the intracellular distribution and organization of actin filaments in transiently transfected HeLa cells. HeLa cells were transfected with the DNA construct encoding ActA(1–584). Cultures of cells were analysed 48 h after transfection. Paraformaldehyde-fixed and detergent-permeabilized cells were fluorescently double-labelled for ActA(1–584) and for F-actin. For immunofluorescence staining of ActA(1–584), affinity-purified polyclonal antibodies directed against a proline-rich repeat of ActA were used as primary antibodies and fluorescein-coupled antibodies as secondary antibodies. For specific staining of F-actin, rhodamine-conjugated phalloidin was added during the incubation with the primary antibodies. Left panels are micrographs of the ActA immunofluorescence. Right panels are micrographs of the corresponding stained F-actin. (**A**) and (**B**) are views obtained by epifluorescence microscopy. (**C–F**) are views obtained by confocal laser scanning microscopy. (C and D): plane of focus 1.2 μm above cell substratum (optical section of 0.2 μm). (E) and (F) correspond to vertical section views of the cell shown in panels C and D. The insert in (F) corresponds to a vertical section view of an untransfected cell. Note the strong F-actin staining distributed throughout the whole cell body in the ActA(1–584)-positive cell and the concentration of rhodamine–phalloidin and immunofluorescence stainings in ruffled membranes of the leading edge. Bars: A = 15 μm; C, E, F insert = 5 μm.

by insertion of an exogenous protein into the inner surface of the plasma membrane. Indeed, HeLa cells transfected with a DNA construct encoding protein A fused in-frame to the K-ras plasma membrane localization signal (Hancock *et al.*, 1991) did not show any modification of actin cytoskeleton organization or cell shape, as visualized in Figure 3G and H. The same result was obtained in CV-1 cells (data not shown).

ActA contains at least two functional sites which cause distinct modifications of the actin cytoskeleton in transfected cells

We used the phenotypic modifications caused by ActA(1–584)–CAAX in transfected cells to determine the functionally relevant portions of ActA. Previous studies suggest that the proline-rich repeats of ActA play an important functional and/or structural role (Pistor *et al.*, 1994; Southwick and Purich, 1994). It has been proposed that this sequence may bind profilin, an actin binding protein supposed to promote actin filament assembly (Theriot *et al.*, 1994). Moreover, the results of *in vitro* experiments with synthetic peptides corresponding to three different sequences of the amino-terminal portion of ActA are in support of a direct interaction between this protein and actin (Vancompernolle and Vandekerckhove, personal communication). Based on these observations, we constructed two ActA–CAAX hybrid proteins, ActA(1–234)–CAAX and ActA(234–584)–CAAX, as well as the corresponding cytoplasmic derivatives ActA(1–234) and ActA(234–584) (see Figure 1).

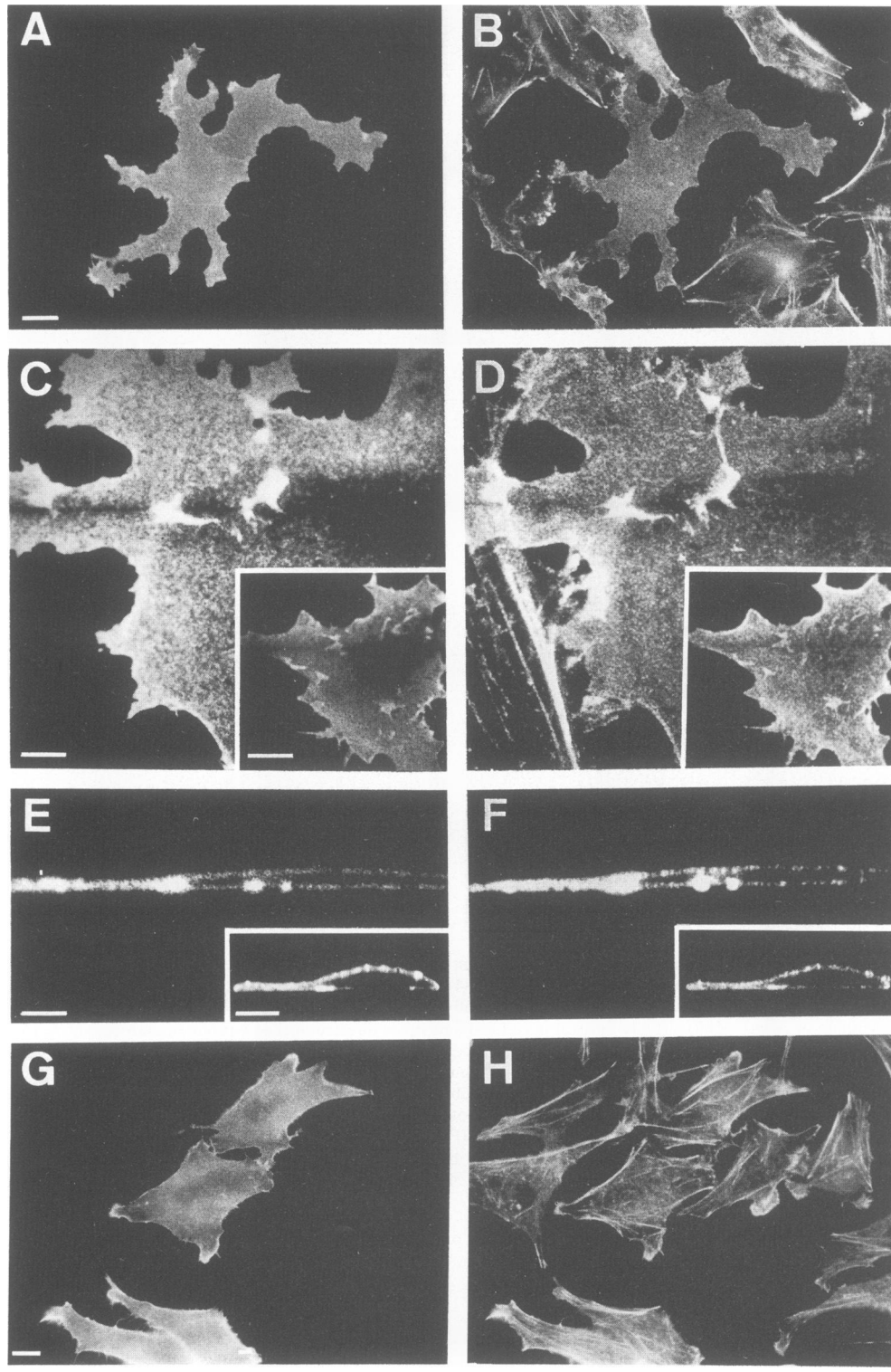

Fig. 3. Effects of membrane-associated ActA(1–584)–CAAX on the organization of the actin cytoskeleton and on the shape of HeLa cells. Cells were transfected with DNA constructs encoding ActA(1–584)–CAAX or protein A–CAAX, used as a control. Cultures of cells were analysed 48 h after transfection. Cells were double-labelled for F-actin and ActA or protein A–CAAX as described in Figure 2, with the exception of the immunofluorescence staining of protein A–CAAX for which purified rabbit IgGs were used as primary antibodies. Left panels are micrographs of the immunofluorescence stainings. Right panels are micrographs of the corresponding phalloidin stainings. (**A, B**): light microscopy images of an ActA(1–584)–CAAX-producing cell. Note the reorganization of the actin cytoskeleton and the modification of cell shape. (**C, D**) and (**E, F**): confocal microscopy images of ActA(1–584)–CAAX-producing cells. (C, D): plane of focus at ventral face of the cells. Inserts in C and D show an overview of an ActA(1–584)–CAAX-positive cell. The bright F-actin staining, which is homogeneously distributed all over the ventral plasma membrane face of the ActA(1–584)–CAAX-producing cells, is lacking in neighbouring untransfected cells which exhibit actin cytoskeletal structures such as stress fibres. (E, F and inserts): vertical section views of the cells shown in C ,D and in inserts; note the co-distribution of F-actin and ActA(1–584)–CAAX labels at the cellular cortex. (**G, H**): protein A –CAAX. Light microscopy images of protein A–CAAX-positive cells, the actin cytoskeleton and shape of which are indistinguishable from those of untransfected neighbouring cells. Bars: A, G = 15 μm; C, E = 5 μm; inserts = 10 μm.

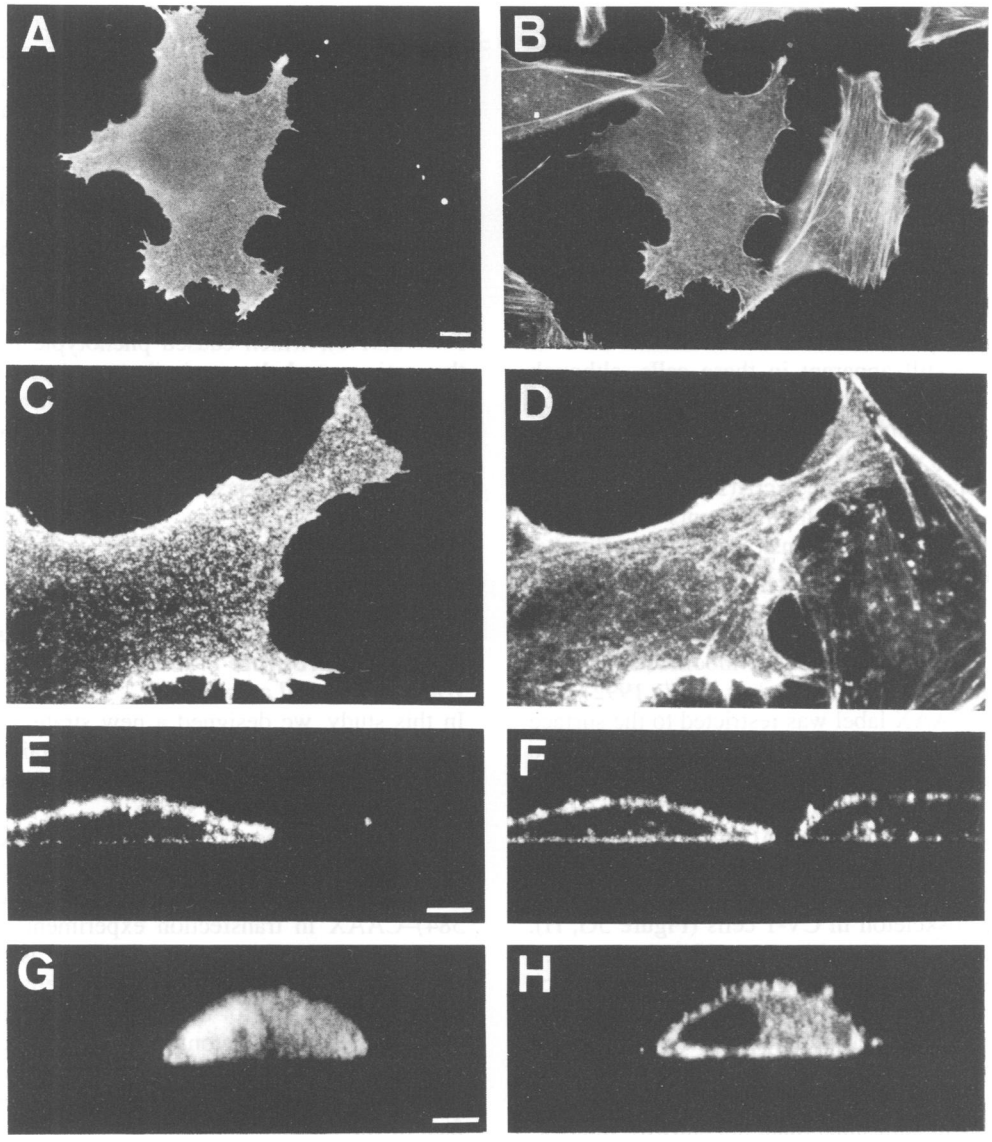

Fig. 4. Effects of ActA(1–234)–CAAX on the intracellular distribution and organization of the actin cytoskeleton in transfected HeLa cells. Cells were transfected with DNA constructs encoding ActA(1–234)–CAAX. Cultures of cells were analysed 48 h after transfection. Cells were double-labelled for F-actin and ActA(1–234)–CAAX as described in Figure 2, with the difference that affinity-purified polyclonal antibodies recognizing a sequence located in the amino-terminal portion of ActA were used as primary antibodies. Left panels are micrographs of the immunofluorescence stainings. Right panels are micrographs of the corresponding phalloidin stainings. (**A, B**): light microscopy images of an ActA(1–234)–CAAX-producing cell. Note the reorganization of the actin cytoskeleton induced by ActA(1–234)–CAAX, which is reminiscent of that caused by ActA(1–584)–CAAX. (**C, D** and **E, F**): confocal microscopy images of an ActA(1–234)–CAAX-producing cell. (C, D): plane of focus at ventral face of the cells. (E, F): vertical section views of the cells shown in C and D; note the increase in F-actin staining at the cellular cortex of the ActA(1–234)–CAAX-producing cell. (**G, H**): vertical section view of a cell producing cytoplasmic ActA(1–234); note the increase in cytoplasmic F-actin staining. Bars: A = 10 μm; C, E, G = 5 μm.

Production of the ActA(1–234)–CAAX construct, which encodes the amino-terminal portion of ActA and which does not include the proline-rich repeats (Figure 1A), induced phenotypic modifications of the actin cytoskeleton in both HeLa and CV-1 cells which were reminiscent of those observed with ActA(1–584)–CAAX. Panels A and B of Figure 4 show a HeLa cell producing this ActA variant. This cell exhibited a pronounced reduction in prominent F-actin structures such as stress fibres, together with a diffuse F-actin staining which was homogeneously distributed all over the cell surface. Images obtained by confocal microscopy revealed an increase in diffuse F-actin staining at the plasma membrane in cells producing ActA(1–234)–CAAX (Figure 4C, D, plane of focus at ventral face of cells; E and F, vertical section views). The distribution of F-actin followed that of ActA(1–234)–CAAX. However, in contrast to cells producing ActA(1–584)–CAAX, those producing ActA(1–234)–CAAX exhibited a reduced number of membrane protrusions, together with retraction of the peripheral plasma membrane which was reminiscent of that observed in cells treated with low amounts of cytochalasin D, a drug which inhibits dynamic actin turnover (Forscher and Smith, 1988; Friederich *et al.*, 1993; for review, see Cooper, 1987). In most of the HeLa cells transfected with the DNA construct encoding ActA(1–234) without the CAAX signal, this ActA variant was detected in the nucleus (data not shown). However, a significant proportion of transfected cells also

exhibited cytoplasmic staining (Figure 4G) which was paralleled by an increase in cytoplasmic F-actin staining (Figure 4H), very similar to that observed in HeLa cells producing ActA(1–584).

In contrast to the effects of ActA(1–234)–CAAX, which were similar in HeLa and CV-1 cells (data not shown), those caused by ActA(235–584)–CAAX, comprising the proline-rich repeats and the carboxy-terminal portion of ActA, were cell type dependent. Most of the HeLa cells producing this ActA variant exhibited little reorganization of the actin cytoskeleton and cell shape. As shown in Figure 5A and B, prominent F-actin structures such as stress fibres were still apparent in these cells, although they seemed less organized. No increase in diffuse F-actin staining at plasma membrane surfaces was observed by confocal microscopy analysis (data not shown). However, a significant proportion of the ActA(235–584)–CAAX-positive cells (10%) producing high amounts of this ActA variant (as indicated by the intensity of immunofluorescence signal; Figure 6D), exhibited circumferential plasma membrane blebbing. These surface modifications, which are illustrated by the confocal microscopy images (Figure 5C–F), are indicative of a structural modification of the cortical actin cytoskeleton (Cunningham *et al.*, 1992). The ActA(234–584)–CAAX label was restricted to the surface of these membrane protrusions (Figure 5C, E) which also reacted with rhodamine–phalloidin (Figure 5D, F). These morphological modifications were not observed in HeLa cells producing cytoplasmic ActA(234–584) (data not shown). In contrast to the effects observed in HeLa cells, ActA(235–584)–CAAX caused a dramatic reorganization of the F-actin cytoskeleton in CV-1 cells (Figure 5G, H). Compared with untransfected cells, which had a well organized stress fibre system, most of the CV-1 cells which produced ActA(235–584)–CAAX accumulated prominent F-actin structures at the cell periphery with low amounts of F-actin in the cell body and in membrane protrusions (Figure 5H). These cells also presented a reduction in well-organized focal adhesions (data not shown). Interestingly, CV-1 cells never exhibited the surface blebbing observed with HeLa cells.

Semi-quantitative evaluation of the F-actin content in cells producing ActA variants

In order to compare quantitatively the F-actin content of cells producing ActA variants with that of untransfected cells, the fluorescence intensities of rhodamine–phalloidin, used at saturating concentrations, were measured (Figure 6). We chose this semi-quantitative approach, which has been successfully used in previous studies (Symons and Mitchison, 1991), because the F-actin content of these transiently transfected cell cultures could not be determined biochemically. On average, the rhodamine fluorescence intensity in ActA(1–584)- or ActA(1–584)–CAAX-positive cells was higher (23 and 60%, respectively, $n = 14$) than in untransfected cells ($n = 14$), suggesting that ActA production leads to an increase in F-actin content. Plasma membrane-associated ActA had a more pronouced effect on the F-actin content than the cytoplasmic ActA variant. Cells which produced ActA(1–234)–CAAX or ActA(235–584)–CAAX also showed higher rhodamine–phalloidin intensities, although to a lesser extent (15 and 10%, respectively, $n = 14$) than cells producing ActA(1–584) or ActA(1–584)–CAAX. The intensity of fluorescein fluorescence associated with immunolabelled ActA variants was measured in parallel for individual cells to determine whether, in a given cell, the F-actin content was correlated with the amount of ActA variant produced. Plotting rhodamine versus fluorescein intensities indicated that the amount of F-actin was proportional to the amount of ActA(1–584) and ActA(1–584)–CAAX (Figure 6A, B, $r = 0.71$ and 0.83, respectively; $P < 0.01\%$). Interestingly, the same correlation was observed for ActA(1–234)–CAAX (Figure 6C, $r = 0.79$; $P < 0.01\%$), which caused phenotypic modifications of the actin cytoskeleton similar to those observed with ActA(1–584)–CAAX. Inversely, there was no statistically significant correlation between phalloidin–rhodamine fluorescence and ActA(235–584)–CAAX-associated fluorescein fluorescence intensities (Figure 6D, $r = 0.189$; $P > 0.1\%$).

Discussion

Cytoplasmic and plasma membrane-associated ActA both promote F-actin assembly in transfected HeLa cells

In this study, we designed a new strategy to analyse the functional properties of ActA and to obtain information on the mechanism of ActA-mediated actin filament nucleation and on its effect on cell shape.

We compared the effects of a cytoplasmic ActA variant, ActA(1–584), and an ActA derivative fused to the K-ras (B) plasma membrane localization sequence, ActA(1–584)–CAAX in transfection experiments. Fusion of the K-ras sequence to ActA caused it to associate with the membrane fraction of transfected cells. Restriction of ActA localization to the dorsal and ventral faces of transfected cells was confirmed by confocal microscopy analysis. Taken together, these findings indicate that ActA(1–584)–CAAX was correctly located on the inner face of the plasma membrane.

Despite their different intracellular localizations, production of either ActA(1–584)–CAAX or ActA(1–584) increased F-actin content, as determined by quantitation of rhodamine–phalloidin fluorescence signals. Thus, ActA may overcome the negative control on actin polymerization which has been demonstrated to exist in eukaryotic cells (Sanders and Wang, 1990; Symons and Mitchison, 1991) and may promote actin polymerization. Since the transient transfection approach did not permit the concentration of total actin in transfected cells to be determined by biochemical approaches, we cannot determine whether the increase in F-actin content is due solely to an increase in the F- to G-actin ratio or whether the total amount of cellular actin has increased.

Localization of ActA to the plasma membrane is paralleled by actin assembly

In HeLa cells, ActA(1–584) was mainly detected in the cytoplasm and induced a large increase in cytoplasmic F-actin staining. In contrast, this ActA variant was predominantly located in the nucleus and caused little increase in cytoplasmic F-actin staining in CV-1 cells. The latter effects were similar to those previously observed with a similar ActA derivative transfected into PtK2 cells (Pistor

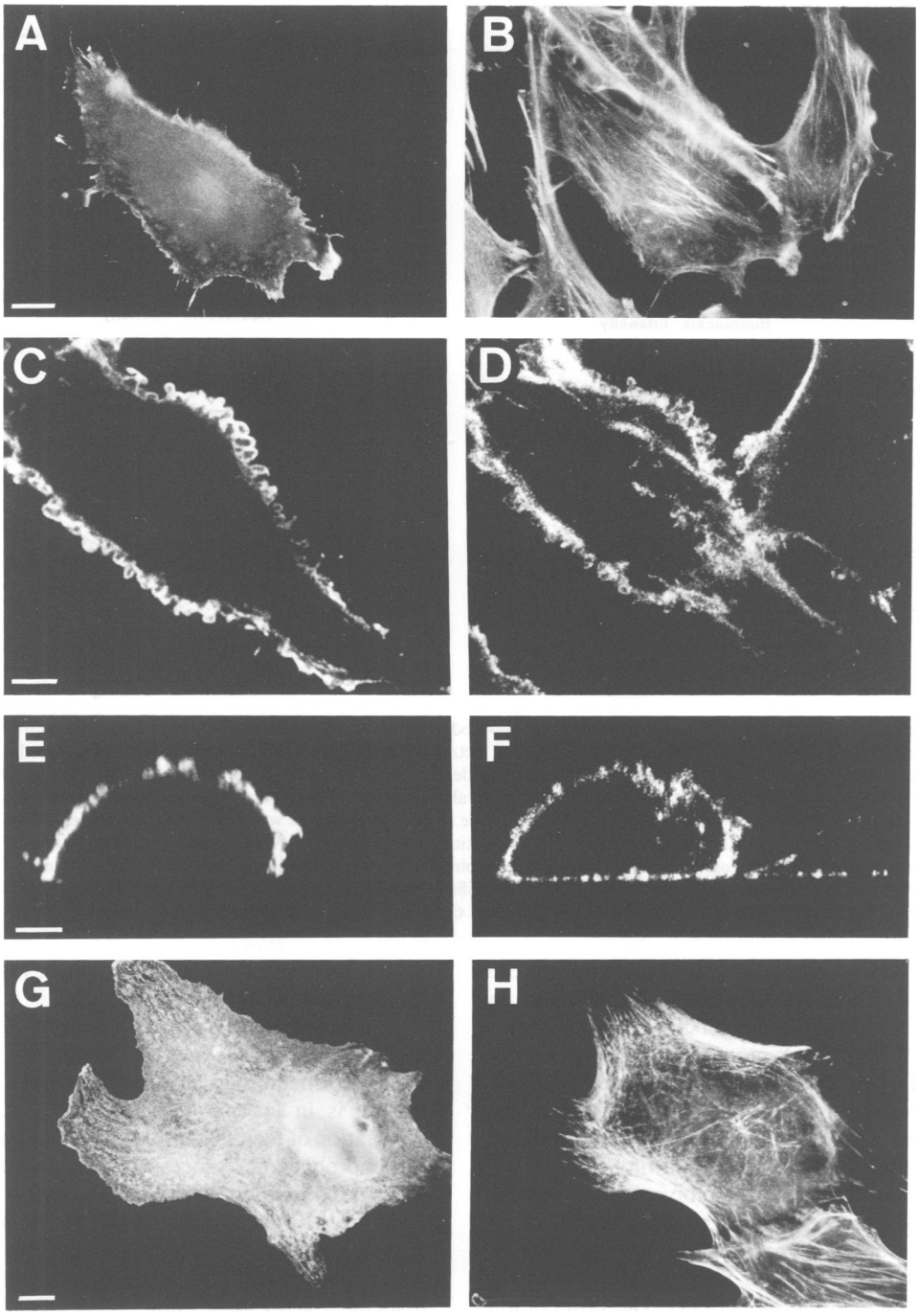

Fig. 5. Effects of ActA(235–584)–CAAX on the organization of the actin cytoskeleton and of cell shape in transfected cells. HeLa (**A–F**) or CV-1 (**G, H**) cells were transfected with a DNA construct encoding ActA(235–584)–CAAX. Cultures of cells were analysed 48 h after transfection. Cells were double-labelled for F-actin and ActA(235–584)–CAAX as described in Figure 2. Left panels are micrographs of the immunofluorescence stainings. Right panels are micrographs of the corresponding phalloidin stainings. (A, B): light microscopy images of an ActA(235–584)–CAAX-producing HeLa cell. (C–F): confocal microscopy images of an ActA(235–584)–CAAX-producing HeLa cell. (C, D): plane of focus at middle of the cell body. The ActA(235–584)–CAAX-producing cell exhibits surface blebbs lined by the immunofluorescence and F-actin labels.
(E, F): vertical section views of the cells shown in C and D. ActA (235–584)–CAAX label is restricted to the dorsal cell face. (G, H): light microscopy images of an ActA(235–584)–CAAX-positive CV-1 cell. In contrast to the untransfected cell, which has organized stress fibres, F-actin structures of the ActA(235–584)–CAAX-producing cell are concentrated at the cell periphery and F-actin label in membrane extensions is reduced. Bars: A, G = 10 μm; C, E = 5 μm.

et al., 1994). These findings suggest that the nuclear location of ActA is dependent on cell type-specific factors. It is not yet clear whether ActA translocates into the nucleus directly or in association with another protein. The accumulation of ActA in the nucleus in some cell types may mean that the level of cytoplasmic ActA remains too low to cause modifications of the actin cytoskeleton. Alternatively, these cells may have a limited amount of the cytoplasmic factor or factors required for ActA-induced actin assembly.

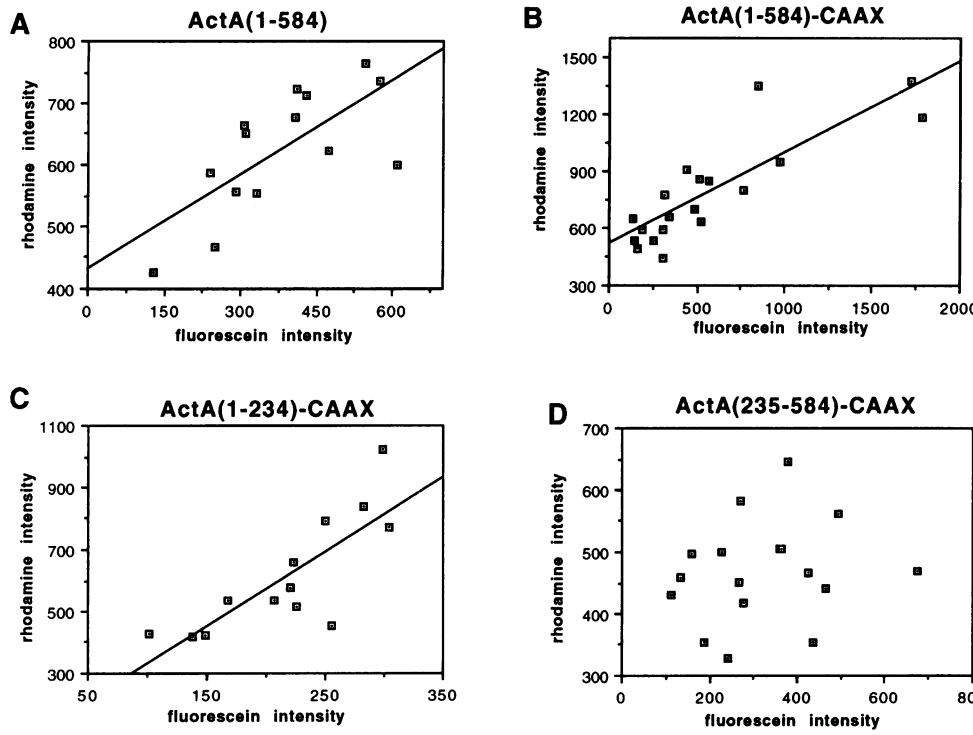

Fig. 6. Semi-quantitative evaluation of F-actin content in ActA variant-producing HeLa cells. HeLa cells were transfected with DNA constructs encoding ActA(1–584), ActA(1–584)–CAAX, ActA(1–234)–CAAX or ActA(235–584)–CAAX. Cultures of cells were analysed 48 h after transfection. Cells were double-labelled for F-actin and ActA variants as described in Figures 2 and 5, with the difference that saturating amounts of phalloidin–rhodamine were used. Optical sections acquired at 2 μm intervals by confocal microscopy were projected to reconstitute the total volume of single cells. The total intensity of fluorescein or rhodamine fluorescence of projected images was calculated. In parallel, the rhodamine–phalloidin intensity of neighbouring untransfected cells was determined. The correlation of the amount of ActA variant produced (fluorescein intensity) with that of the F-actin content (rhodamine intensity) is represented in the graphs. For each transfected cell the phalloidin–rhodamine intensity was plotted as a function of the fluorescein intensity. (**A**) ActA(1–584); (**B**) ActA(1–584)–CAAX; (**C**) ActA(1–234)–CAAX; (**D**) ActA(235–584)–CAAX. Note that the increase in intensity of ActA(235–584)–CAAX–fluorescein is not correlated to that of rhodamine–phalloidin.

While ActA(1–584) induced actin assembly in the cytoplasm of HeLa cells, ActA(1–584)–CAAX led to an increase in F-actin staining at the dorsal and ventral faces of cells, indicating that ActA promotes F-actin assembly when associated with the plasma membrane. Previous studies demonstrated that actin filaments assemble at the plasma membrane and depolymerize in the cell body (Forscher and Smith, 1988; Symons and Mitchison, 1991). It has been proposed that actin assembly occurs preferentially at the cellular cortex, because proteins that promote actin polymerization are specifically recruited to the plasma membrane (Hartwig and Shelvin, 1986; Hartwig *et al.*, 1989; Guiliano and Taylor, 1994). The observation that actin assembly occurs in the cytoplasm or at the plasma membrane in transfected cells, depending on the intracellular localization of ActA, is in favour of such a mechanism.

Plasma membrane association of ActA is required for the formation of plasma membrane extensions

Although cytoplasmic ActA(1–584) caused a redistribution of F-actin and the disassembly of stress fibres, neither the overall cell shape nor actin assembly in polarized membrane protrusions and ruffles was affected. These observations suggest that, despite the accumulation of cytoplasmic ActA(1–584) in these membrane structures, endogenous, spatially controlled actin assembly was not grossly modified. Thus the depolymerization of actin structures such as stress fibres may be caused by mass action, resulting from the recruitment of actin monomers by cytoplasmic ActA(1–584).

In contrast to cells which produced cytoplasmic ActA, those which synthesized the membrane-associated ActA variant formed broad lamellar membrane extensions. This finding is in favour of the idea that plasma membrane association of factors involved in actin assembly is required for morphogenic processes. The homogeneous, non-polarized distribution of F-actin suggests that ActA(1–584)–CAAX may interfere with the spatial control of actin polymerization. Thus, it is conceivable that this ActA variant competes with endogenous plasma membrane-associated actin nucleators.

Dynamic turnover of submembranous actin filaments, a process which has been shown to be intimately linked to the formation of membrane protrusions in normal cells (Forscher and Smith, 1988; Theriot and Mitchison, 1991) and which occurs in the tail-like F-actin structure of *Listeria* (Theriot *et al.*, 1992), may also be required for the formation of membrane extensions in ActA(1–584)–CAAX-producing cells. In addition, it is conceivable that the morphological modifications observed in cells producing this ActA variant result from a reorganization of the cortical actin lattice. Nucleation of a large number of short actin filaments by ActA may modify the mechanical tension of the cortical actin network and result in its weakening, which favours the formation of membrane protrusions (Ingber, 1993). Intracellular *Listeria* form membrane protrusions when they reach the plasma

membrane of host cells (Tilney and Portnoy, 1989). Although, in the present study, ActA is directly associated with the plasma membrane, the mechanisms proposed here may also participate in the formation of *Listeria*-containing filopodia in infected cells. Despite the fact that cells producing membrane-associated ActA had less well organized focal contacts, they were extremely well spread. This observation suggests that a redistribution of tractional forces on cell adhesion sites may be a consequence of the redistribution of focal adhesion-associated proteins. In this regard, it is interesting to note that some of these proteins are also recruited into the tail-like F-actin structure of *Listeria* (Dold *et al.*, 1994). The phenotypic modifications observed with membrane-bound ActA were specifically related to this protein since they were not detected in cells producing membrane-associated protein A.

Towards a model of action for ActA: after nucleation by the amino-terminal portion of ActA, actin assembly is driven by a mechanism which requires the remaining portion of the protein including the proline-rich repeats

The interpretation of previous results obtained with ActA deletion variants was difficult because these variants were inactive in transfection assays (Pistor *et al.*, 1994). In contrast to this, both of the shorter ActA derivatives analysed here had distinct effects on the organization of the actin cytoskeleton and on cell morphology. It is of particular interest that ActA(1–234)–CAAX, which includes the amino-terminal portion of ActA, induced a redistribution of F-actin very similar to that observed with ActA(1–584)–CAAX, as well as a significant increase in F-actin content which was proportional to the amount of protein produced. These findings strongly suggest that the amino-terminal portion of ActA may promote actin assembly. Since *Listeria* bacteria do not nucleate actin assembly efficiently *in vitro* (Tilney *et al.*, 1992b) and ActA has so far not been found to bind actin *in vitro* (Kocks *et al.*, 1992), it is not yet clear whether ActA(1–234)–CAAX recruits actin directly or whether it binds a nucleating factor. Evidence for a direct interaction with actin was obtained in a recent study which demonstrated that three synthetic peptides corresponding to amino-proximal segments of ActA bind actin *in vitro* and affect the organization of the actin cytoskeleton (Vancompernolle and Vandekerckhove, personal communication). It is conceivable that binding of the amino-terminal portion of ActA to actin is regulated by an as yet unknown mechanism which requires factors present in the host cell cytosol.

In contrast to the effects of the amino-terminal portion of ActA, those observed with ActA(235–584)–CAAX, which comprises the remaining portion of ActA including the proline-rich repeats, differed depending on the cell type used for transfection. Moreover, although ActA(235–584)–CAAX increased the F-actin content slightly in transfected cells, there was no correlation between the amounts of F-actin and the ActA variant. These findings are in support of an indirect mechanism of action for ActA(235–584)–CAAX. It is of interest that ActA(1–234)–CAAX, which contains the potential nucleation site, did not induce the formation of membrane protrusions, a process which involves dynamic actin turnover. ActA(234–584)–CAAX might interfere with factor(s) which participate(s) in the control of actin assembly. Such a mechanism would account for the plasma membrane blebbing observed in transfected HeLa cells and for the reorganization of the actin cytoskeleton in CV-1 cells. Data obtained in immunolocalization studies of profilin in *Listeria*-infected cells and upon profilin depletion of oocyte extracts suggest that profilin may be one of these factors (Theriot *et al.*, 1994). Profilin co-distributes with ActA at the rear of the bacteria and is required for tail formation and bacterial movement (Theriot *et al.*, 1994; for reviews, see Machesky and Pollard, 1993; Sohn and Goldschmidt-Clermont, 1994). While the mechanism of action of profilin in cells is not yet clear, it is well documented that profilin causes reorganization of the actin cytoskeleton in a condition-dependent manner (Haarer *et al.*, 1990; Cao *et al.*, 1992; Finkel *et al.*, 1994). It is noteworthy that ActA(235–584)–CAAX production in CV-1 cells caused a redistribution of prominent F-actin structures, such as stress fibres, which was very similar to that observed after microinjection of profilin into cultured Ptk-2 cells (Cao *et al.*, 1992). However, our experimental system did not allow us to detect a significant increase in the amount of plasma membrane-associated profilin in cells producing ActA(1–584)–CAAX (as assessed by immunostaining with human profilin-specific antibodies; data not shown). The redistribution of profilin over the large plasma membrane surface may result in a low concentration of profilin, making it difficult to detect quantitative changes in the membrane-associated pool of this protein. Another possibility is that proteins with SH3 domains might bind to the polyproline region of ActA to regulate its activity.

Our findings are consistent with a model in which the amino-terminal part of ActA is involved in the nucleation of actin filaments while the segment including the proline-rich repeat region promotes or controls polymerization. The present assay will be a useful tool to test these hypotheses and to further dissect the functionally important sequences of ActA. Moreover, it will be of interest to study the motility of ActA–CAAX-producing cells. Finally, the observation that ActA is able to act as an actin filament nucleator and to cause morphological changes when associated with the inner face of the plasma membrane, raises the question of whether protein(s) with properties similar to those of ActA exist in eukaryotic cells. The isolation and characterization of such protein(s) would be an important step in the understanding of the regulation of actin dynamics.

Materials and methods

Antibodies and fluorochrome-coupled reagents

The affinity-purified ActA-specific polyclonal IgGs directed against a peptide comprising part of the first proline-rich repeat were prepared as previously described by Kocks *et al.* (1993). The ActA-specific polyclonal IgGs were directed against a peptide comprising residues 1–18 of mature ActA (Kocks *et al.*, 1992). The synthetic peptide A18K (5 mg; ATDSEDSSLNTDENEEEK, Neosystem, Strasbourg, France) was coupled with glutaraldehyde to bovine serum albumin (BSA). Then, 125 μg of the conjugate was emulsified with complete Freund's adjuvant and injected into the paw of the rabbit. A boost with the same amount of antigen in incomplete Freund's adjuvant was injected into the paw after 6 weeks, a second boost with the same preparation was injected intramuscularly after 8 weeks, and a third boost without adjuvant was administered intravenously after 10 weeks. The antiserum was affinity-purified using EAH–Sepharase 4B (Pharmacia) coupled to the peptide,

according to the manufacturer's instructions. Anti-peptide antibodies were eluted with 0.1 M glycine (pH 2.5), dialysed against phosphate buffer and stored in phosphate buffer/50% glycerol. The affinity-purified antibody was specific for ActA as determined by immunoblotting of extracts prepared with wild-type and ActA$^-$ mutant bacteria and by immunofluorescence. The antibody was used at a concentration of 1 and 10 μg/ml, for immunoblotting and immunofluorescence, respectively. The monoclonal anti-human vinculin antibody was a kind gift from Dr B.Geiger (Weizmann Institute of Science, Rehovot, Israel). The affinity-purified human profilin-specific polyclonal IgGs were kindly provided by Dr P.J.Goldschmidt-Clermont (Johns Hopkins University School of Medicine, Baltimore, MD, USA). Fluorescein-linked donkey anti-rabbit IgG antibodies and Texas red-coupled sheep anti-mouse IgG antibodies were purchased from Amersham Corp. (Arlington Heights, IL, USA). Rhodamine-coupled phalloidin was purchased from Sigma Chemical Company (St Louis, MO, USA)

Cell lines

The human cervix carcinoma HeLa cell line (ATCC CCL2) and the fibroblast-like monkey kidney cell line CV-1 (ATCC CL 101) were grown in Dulbecco's minimum essential medium (DMEM) supplemented with 10% fetal calf serum (complete medium), at 37°C, under 10% CO_2.

Construction of eukaryotic expression vectors containing actA gene mutants

Standard procedures as described by Sambrook *et al.* (1989) were used for DNA engineering. Base pair positions indicated in the description of the construction of *actA* gene mutants correspond to the *L.monocytogenes* lecithinase operon sequence which comprises the *actA* gene (Vazquez-Boland *et al.*, 1992, see also Figure 1). All DNA fragments obtained by amplification using the polymerase chain reaction were verified by sequencing. Mutants of the *actA* gene were inserted into the eukaryotic expression vector pCB6 (a kind gift of Dr M.Roth, University of Texas, Southwestern Medical Center, Dallas, TX, USA), downstream of the cytomegalovirus promoter.

The DNA construct encoding the protein A–p21$^{kras(B)}$ hybrid protein was kindly provided by Dr J.F.Hancock (ONYX Pharmaceuticals, Richmond, CA, USA). This construct comprises the SV40 virus-derived expression vector pEXV3 (Miller and Germain, 1986) in which has been inserted the sequence encoding bacterial protein A fused in-frame at its 3′ end to that encoding the 17 carboxy-terminal residus of K-ras (B) (Hancock *et al.*, 1991).

Deletion of the actA gene sequences encoding the signal peptide and the bacterial membrane anchorage region. Deletion of the DNA sequence encoding the signal peptide was performed using the PCR technique on a pBR322 derivative in which the complete *actA* gene coding sequence had been inserted into the *Hin*dIII site (p*actA*3, Kocks *et al.*, 1992). The two primers used for the PCR had the following sequence: 5′-CCCAAGGTCCATGGTTGCGACAGATAGCGAA-3′ and 5′-GGGAA-TTCGCATGCTAGAATCTA-3′. The sense primer corresponded to the *actA* gene coding sequence, positions 315–329 of the lecithinase operon (underlined), and comprised a 5′ 'add-on' sequence containing a eukaryotic consensus sequence for translation initiation. The antisense primer was complementary to a sequence of the *actA* gene (positions 793–807) and contained an 'add-on' sequence comprising an *Eco*RI site. One microgram of DNA was used as a template. The concentration of the 5′- and 3′-specific primers was 100 pmol. Twenty four cycles with 1 min denaturation at 94°C, 1 min annealing at 55°C and 1 min extension at 72°C were performed. The resulting amplified fragment of ~480 bp, which comprised the 5′ end of the *actA* gene coding sequence (bp 315–807) was digested with *Eco*RI and inserted into *Eco*RI–*Sma*I-digested pSp64, yielding pSp64–*actA* (315–807).

In order to modify the carboxy-terminal region of the ActA protein, the *actA* gene cloned in the *Hin*dIII site of the pBR322 (p*actA*1) was digested with *Bst*NI. The 5′-overlapping end of the *Bst*NI sites of the resulting mixture of DNA fragments were filled-in using the Klenow fragment of DNA polymerase I. After heat inactivation of the enzyme, the DNA was digested with *Sph*I, and an ~1.2 kb *Sph*I–*Bst*NI blunt-ended *actA* gene fragment (bp 803–2051) was isolated. Finally, a DNA adaptor molecule was synthesized to reconstitute amino acids 580–584 of the ActA protein sequence and to fuse the *actA* gene sequence in-frame to the sequence encoding the carboxy-terminus of K-ras. The two oligonucleotides which formed this adaptor were: 5′-AGCTTCCCGGG-AACCATACGACG-3′ and 5′-AATTCGTCGTATGGTTCCCGGGA-3′. In the adaptor molecule the *actA* gene sequence (bp 2052 –2066) was flanked at the 5′ end by a *Hin*dIII and a *Sma*I site, and at the 3′ end by an *Eco*RI site. First, the adaptor was inserted into a *Hin*dIII–*Eco*RI-digested pBR322. Then, the *Sph*I-digested and *Bst*NI-blunt-ended 1.2 kb *actA* gene fragment (bp 803–2051) was inserted into this construct by ligation through the *Sph*I site of pBR322 and the *Sma*I site of the adaptor. Blunt-end ligation through the *Bst*NI–*Sma*I sites fused the 1.2 kb *actA* gene fragment in-frame to the *actA* sequence of the adaptor encoding amino acids 577–584 of the ActA protein. The resulting construct was named pBR322–*actA*(803–2066) and comprised bp 803–2066 of the *actA*-coding sequence.

In order to reconstitute the 5′ end of the coding region of the *actA* gene, the pBR322–*actA*(803–2066) construct was digested with *Sph*I (cutting at base pair position 803 of the *actA* gene) and *Sal*I (cutting pBR322). The larger ~6 kb fragment which contained almost the entire pBR322 sequence as well as part of the *actA* gene coding region (bp 803–2066) was isolated. The previously modified 5′ end of the *actA* gene was removed after *Sph*I–*Sal*I digestion from the Sp64–*actA*(315–807) construct and ligated to the *Sph*I–*Sal*I-digested 6 kb fragment. The resulting construct comprised the *actA* bases 315–2066, which encode amino acids 1–584 of mature, wild-type ActA. The amino acid sequence of this variant starts with M, V followed by amino acid 1 of the mature ActA protein. For expression in eukaryotic cells, the modified *actA* sequence was removed from pBR322–*actA*(315–2066) by *Eco*RI–*Xba*I digestion. The isolated *actA* gene fragment was inserted into *Xba*I–*Eco*RI-digested pCB6 expression vector, downstream of the cytomegalovirus promoter. An in-frame stop codon was present at the 3′ end of the *actA*-coding region, 21 bp downstream of the *Eco*RI site, resulting in the addition of seven amino acids (D, P, R, V, A, S, L) to the carboxy-terminus of the ActA sequence. This DNA construct was called pCB6–*actA*1 and encoded the ActA variant ActA(1–584).

Fusion of the K-ras (B) plasma membrane localization signal to the carboxy-terminus of ActA(1–584). In order to generate an ActA variant which localizes to the inner surface of the plasma membrane, the 17 carboxy-terminal amino acids of K-ras (B) were fused to the carboxy-terminus of the cytoplasmic ActA(1–584) variant. This sequence has been demonstrated to be sufficient to anchor proteins permanently into the plasma membrane (Hancock *et al.*, 1991; Leevers *et al.*, 1994; Stokoe *et al.*, 1994). An ~160 bp DNA fragment comprising the sequence encoding the 17 carboxy-terminal amino acids of K-ras (SKDGKKKKKSKTKCVIM) as well as ~50 bp of the K-ras 3′-untranslated region was removed from p147 (Hancock *et al.*, 1991) by *Eco*RI digestion. This DNA fragment was inserted into the *Eco*RI-digested and dephosphorylated pCB6–*actA*1 construct, downstream of the 3′ end of the *actA*-coding sequence, giving rise to pCB6–*actA*2. The orientation of the fragment was determined by digestion with asymmetrically located restriction sites. The in-frame ligation of the 3′ end of the *actA*-coding sequence to the 5′ end of the K-ras sequence through the *Eco*RI site generated a chimeric protein called ActA(1–584)–CAAX. The *actA*2 DNA construct was also inserted into the *Xba*I site of pUHD-10-3 (Gossen and Bujard, 1992), which contains a promotor which is inducible by tetracycline when co-transfected with a plasmid producing the bacterial tetracycline repressor fused to the viral V1 enhancer, giving rise to pUHD-10-3–*actA*2.

Construction of the ActA(235–584)–CAAX chimera. In order to delete the *actA* gene sequence encoding the hydrophilic domain upstream from the proline repeat region, two primer oligonucleotides were synthesized. The sense primer (5′-TCCCCGCGGAAGCTTACCATGGTTGACTT-CCCGCCA-3′) comprised *Sac*II and *Hin*dIII sites, followed by the eukaryotic consensus sequence for translation initiation and the *actA* gene sequence (bp 1018–1029, underlined). The antisense primer (5′-ACCCGCATTTC-3′) was complementary to the *actA* gene sequence (bp 1538–1550). The pBR322 derivative p*actA*1 was used as template. DNA amplification was performed using the conditions described above. The amplified ~600 bp DNA fragment was digested with *Sac*II and *Acc*I and the larger ~450 bp fragment comprising the *actA* sequence from bp 1017 to 1411 was purified. The pUHD-10-3–*actA*2 construct was digested with *Sac*II and *Acc*I which cleave the pUHD-10-3 polylinker and the unique *Acc*I site of the *actA* gene, respectively. An ~1100 bp *Sac*II–*Acc*I DNA fragment, comprising the *actA* sequence from bp 315 to 1411, was removed and replaced by the ~450 bp *Sac*II–*Acc*I PCR DNA fragment which contained the eukaryotic translation start site followed by the *actA* sequence from bp 1017 to 1411. The resulting construct, named pUHD-10-3–*actA*3, encodes the ActA variant ActA(235–584)–CAAX which comprises amino acids 235–584 of ActA fused to the 17 carboxy-terminal amino acids of K-ras. The *actA*3 DNA was removed from this vector by digestion with *Hin*dIII–*Xba*I and inserted into pCB6, yielding pCB6–*actA*3.

Construction of the ActA variant ActA(235–584). In order to generate an ActA variant comprising amino acids 235–584 but lacking the K-ras sequence, the pCB6–*actA*3 construct was digested with *Hin*dIII and *Eco*RI. An ~1000 bp fragment which comprised the eukaryotic start of translation followed by the *actA* sequence from bp 1017 to 2066 was inserted into *Hin*dIII–*Eco*RI-digested pCB6, yielding pCB6–*actA*4. Translation of the *actA* sequence was terminated in this construct as described for pCB6–*actA*1. This construct encoded the ActA variant ActA(235–584).

Contruction of the chimera ActA(1–234)–CAAX. In order to construct a recombinant DNA encoding the first hydrophilic domain of ActA followed by the K-ras sequence, two primer oligonucleotides were synthesized. The sense primer 5′-TCCCGCGGGGTGGCATGCAGT-CAG-3′ comprised a sequence of the *actA* gene (bp 802–813, underlined) and a *Sac*II site. The antisense primer 5′-CCCGAATTCCGAA-GCATTTAC-3′ comprised a sequence complementary to the *actA* gene (bp 1011–1016) and an *Eco*RI site. The PCR product obtained after amplification as described above corresponded to the *actA* sequence from bp 802 to 1016 and was digested with *Eco*RI–*Sac*II. The pUHD-10-3–*actA*2 construct encoding ActA(1–584)–CAAX was digested with *Sac*II and *Eco*RI, which cleave the polylinker of the vector upstream of the *actA* sequence and at the junction of the *actA*/K-ras sequences, respectively. The larger *Sac*II–*Eco*RI DNA fragment corresponding to the pUHD-10-3 vector which comprised the sequence encoding the 17 carboxy-terminal amino acids of K-ras was ligated to the purified *Sac*II–*Eco*RI-digested PCR DNA fragment, yielding pUHD-10-3–*actA*(803–1016–ras). In this construct, the *actA* sequence was fused through the *Eco*RI site in-frame to the K-ras sequence. In order to generate a construct encoding amino acids 1–234 of ActA, the pUHD-10-3–*actA*2 construct encoding ActA(1–584)–CAAX was digested with *Sac*II and *Sph*I, which cleave the polylinker of the vector and at the unique *Sph*I site of the *actA* coding region, respectively. An ~500 bp DNA fragment corresponding to the modified 5′ end of *actA* (bp 315–802) was purified and ligated into the *Sac*II–*Sph*I-digested pUHD-10-3–*actA*(803–1016–ras) construct, yielding pUHD-10-3–*actA*5. This construct encodes the ActA variant ActA(1–234)–CAAX, which starts with the amino acids M, V, followed by amino acids 1–234 of ActA and the 17 carboxy-terminal amino acids of K-ras. The *actA*5 DNA fragment was removed from pUHD-10-3 by *Xba*I digestion and inserted in to *Xba*I-cut pCB6, yielding pCB6–*actA*5.

Construction of the ActA variant ActA(1–234). In order to generate an ActA variant comprising amino acids 1–234 but lacking the K-ras sequence, the pCB6–*actA*5 construct was digested with *Xba*I–*Eco*RI. An ~700 bp fragment which comprised the eukaryotic translation start site followed by the *actA* sequence bp 315 to 1016 was inserted into *Xba*I–*Eco*RI-digested pCB6 vector, yielding pCB6–*actA*6. Translation of the *actA* sequence was terminated in this construct as described for pCB6–*actA*1. This construct encoded the ActA variant ActA(1–235).

DNA sequencing

Double-stranded templates containing the mutagenized DNAs were used. DNA sequencing was performed with a Sequenase 2.0 kit (US Biochemical Corp.).

Transient DNA expression in cultured cells

HeLa or CV-1 cells were transfected using the calcium phosphate DNA precipitation method (Matthias *et al.*, 1983). Routinely, 5 μg of DNA was added to cells plated on glass coverslips in 35 mm dishes. Cells were analysed 24–48 h after addition of DNA.

Immunoblotting

Transfected cells plated on 3.5 cm culture dishes were processed for immunoblotting as previously described (Friederich *et al.*, 1989). One tenth of each cell lysate was used for immunoblot analysis. Proteins were separated by SDS–polyacrylamide gel electrophoresis under reducing conditions (Laemmli, 1970). Transfer on nitrocellulose and antibody incubations were performed according to the method described by Burnette (1981) and modified as previously described (Coudrier *et al.*, 1983). Affinity-purified polyclonal ActA-specific antibodies (10 μg/ml) were used as the first antibodies.

Cell fractionation

Six 10 cm dishes of HeLa cells were transfected with DNA constructs (20 μg) encoding ActA(1–584) or ActA(1–584)–CAAX as described above and analysed after 36 h. Cells were washed twice with PBS, scraped off the dish with a rubber policeman and pelleted by centrifugation at 100 *g*. Cells were fractionated into a cytosolic and a crude membrane fraction according to a modification of the procedure described by Hancock and co-workers (1991). Cells were resuspended in 1 ml hypotonic lysis buffer (50 mM Tris–HCl pH 7.5, 5 mM $MgCl_2$, 1 mM DTT, 0.25 M sucrose) and lysed by several passages through a 'cell cracker' at 4°C. The lysate was centrifuged for 10 min at 10 000 *g* and the resulting post-nuclear supernatant was centrifuged for 1.5 h at 100 000 *g*. The supernatant was acetone precipitated for 2 h at –20°C. The precipitated cytosol as well as the membrane pellet were resuspended in 100 μl of lysis buffer and equal proportions of the fractions were used for immunoblotting analysis as described above.

Phosphatase treatment of cell lysates

HeLa cells transfected with a DNA construct encoding ActA(234–584)–CAAX were processed as described for immunoblotting. The lysate was diluted five times in a buffer containing 1 mM $ZnCl_2$ and 10 mM Tris–HCl, pH 7.5, and incubated for 2 h at 37°C in the absence or presence of 20 U of calf intestinal phosphatase (Boerhinger, Mannheim, Germany). After incubation, samples were analysed by immunoblotting.

Fluorescent labelling of the cells

In general, transfected cells were fixed with 3% paraformaldehyde, detergent permeabilized with 0.4% Triton-X100 and labelled as described (Reggio *et al.*, 1983). For immunofluorescence staining of ActA, cells were incubated with affinity-purified polyclonal anti-ActA antibodies (10 μg/ml) and then with rabbit IgG-specific antibodies conjugated to fluorescein (Amersham). In order to visualize F-actin, rhodamine-conjugated phalloidin (Sigma; 0.1 μg/ml) was added to the anti-ActA antibodies. For double-labelling of ActA and vinculin, the ActA-specific antibody was mixed with a human vinculin-specific antibody. Cells were stained with secondary antibodies specific for mouse or rabbit IgGs, coupled to Texas red or fluorescein respectively. The cross-reactivity of secondary antibodies was checked by incubating *actA* DNA-transfected cells with anti-ActA or anti-vinculin antibodies followed by an incubation with anti-mouse IgG-specific antibodies in the first case and anti-rabbit IgG-specific antibodies in the latter case.

Laser scanning confocal microscopy and quantitation of fluorescence

HeLa cells were transiently transfected with *actA* DNA constructs encoding ActA variants. After 28 h, cellular ActA and F-actin were labelled as described above, except that rhodamine–phalloidin was added at saturating concentrations (1 μg/ml).

Cells were analysed using a confocal laser scanning microscope (Leica Instruments Gmbh Heidelberg, Germany) equipped with an argon–krypton laser operating in multi-line mode. Cell preparations, double-labelled with rhodamine and fluorescein conjugates, were sequentially analysed to avoid the overlapping of the fluorescence emission profiles. The excitation line for rhodamine was 568 nm and emission was detected through a long wave pass filter OG590. Fluorescein was excitated with the 488 nm line and emission was detected through a narrow band filter centered at 535 ± 8 nm.

Quantitation of the fluorescence intensities and determination of the cell surface were performed using software established by Leica Instruments. All recorded fields were analysed using a 25× /NA 0.75 objective. The conditions for excitation and detection were adjusted on the most fluorescent sample and remained almost constant during recording. Under these conditions, the fluorescence intensity varied linearly from 0 to 255 for each fluochrome. The pixel size was 0.8 × 0.8 μm, close to the optical resolution. Optical sections at 2 μm intervals were acquired from the substratum contact site of the cell to its top. To determine total fluorescence of single cells, fluorescence intensities of all optical sections were summed up for each cell. For comparison of rhodamine intensities of cells producing ActA and untransfected cells, fields recorded on the same coverslip were analysed. Graphs representing the correlation of fluorescein and rhodamine intensities were obtained using a Criquet software programme. The linear correlation coefficient r was calculated by the same programme. The statistical table established by Fisher and Yates was used to determine the probability value for the correlation coefficient r (Schwartz, 1963).

In order to determine the surface of single cells, a reconstruction of the cell volume was performed using all recorded sections. The cell form was delimited by a precise drawing and the surface was calculated.

Acknowledgements

We wish to thank Dr Pascal Goldschmidt-Clermont for the gift of antibodies against human profilin and Dr Benjamin Geiger for providing

us with antibodies against human vinculin. We are indepted to Dr J.F.Hancock for the gift of the pEXV3–protein A–CAAX expession construct. Thanks are also due to Dr Tony Pugsley for careful reading of the manuscript and for his constructive comments. We would like to express our appreciation to Jean-Claude Benichou for his help with the photographic work. This work was supported by grants from the Association pour la Recherche sur le Cancer (ARC-N°6379), the Fondation pour la Recherche Médicale and the Ligue Nationale Française contre le Cancer and from the Institut National de la Santé et de la Recherche Médicale (CRE 93013) and the DRET (93–109).

References

Brundage,R.A., Smith,G.A., Camilli,A., Theriot,J.A. and Portnoy,D.A. (1993) *Proc. Natl Acad. Sci. USA*, **90**, 11890–11894.

Burnette,W.N. (1981) *Anal. Biochem.*, **112**, 195–203.

Cao,L.-G., Babcock,G.G. and Rubenstein,P.A. (1992) *J. Cell Biol.*, **117**, 1023–1029.

Cooper,J.A. (1987) *J. Cell Biol.*, **105**, 1473–1478.

Cossart,P. (1995) *Curr. Opin. Cell Biol.*, **7**, 94–101.

Cossart,P. and Kocks,C. (1994) *Mol. Microbiol.*, **13**, 395–402.

Coudrier,E., Reggio,H. and Louvard,D. (1983) *EMBO J.*, **2**, 469–475.

Cunningham,C.C., Gorlin,J.B., Kwiatkowski,D.J., Hartwig,J.H., Janmey, P.A., Byers,H.R. and Stossel,T.P. (1992) *Science*, **255**, 325–327.

Dabiri,G.A., Sanger,S.M., Portnoy,D.A. and Southwick,F.S. (1990) *Proc. Natl Acad. Sci. USA*, **87**, 6068–6072.

DeBiasio,R.L., Wang,L.-L., Fisher,G.W. and Taylor,D.L. (1988) *J. Cell Biol.*, **107**, 2645–2631.

Dold,F.G., Sanger,J.M. and Sanger,J.W. (1994) *Cell Motil. Cytoskeleton*, **28**, 97–107.

Domann,E., Wehland,J., Rohde,M., Pistor,S., Hartl,M., Goebel,W., Leimeister-Wächter,M., Wueschner,M. and Chakraborty,T. (1992) *EMBO J.*, **11**, 1981–1990.

Finkel,T., Theriot,J.A., Dise,K.R., Tomaselli,G.F. and Goldschmidt-Clermont,P.J. (1994) *Proc. Natl Acad. Sci. USA*, **91**, 1510–1514.

Forscher,P. and Smith,S.J. (1988) *J. Cell Biol.*, **107**, 1505–1516.

Forscher,P., Lin,C.H. and Thompson,C. (1992) *Nature*, **357**, 515–518.

Friederich,E., Huet,C., Arpin,M. and Louvard,D. (1989) *Cell*, **59**, 461–475.

Friederich,E., Kreis,T.E. and Louvard,D. (1993) *J. Cell Sci.*, **105**, 765–775.

Gossen,M. and Bujard,H. (1992) *Proc. Natl Acad. Sci. USA*, **89**, 5547–5551.

Guiliano,K.A. and Taylor,D.L. (1994) *J. Cell Biol.*, **124**, 971–983.

Haarer,B.K., Lillie,S.H., Adams,A.E.M., Magdolen,V., Bandlow,W. and Brown,S.S. (1990) *J. Cell Biol.*, **110**, 105–114.

Hancock,J.F., Paterson,H. and Marshall,C.J. (1990) *Cell*, **63**, 133–139.

Hancock,J.F., Cadwallader,K., Paterson,H. and Marshall,C.J. (1991) *EMBO J.*, **10**, 4033–4039.

Hartwig,J.H. and Shelvin,P. (1986) *J. Cell Biol.*, **103**, 1007–1020.

Hartwig,J.H., Chambers,K.A., Hopcia,K.L. and Kwiatkowski,D.J. (1989) *J. Cell Biol.*, **109**, 1571–1579.

Hitt,A.L., Lu,T.H. and Luna,E.J. (1994a) *J. Cell Biol.*, **126**, 1421–1431.

Hitt,A.L., Hartwig,J.H. and Luna,E.J. (1994b) *J. Cell Biol.*, **126**, 1433–1444.

Hubbard,A.L. and Ma,A. (1983) *J. Cell Biol.*, **96**, 230–239.

Ingber,D.E. (1993) *J. Cell Sci.*, **104**, 613–627.

Kocks,C., Gouin,E., Tabouret,M., Berche,P., Ohayon,H. and Cossart,P. (1992) *Cell*, **68**, 521–531.

Kocks,C., Hellio,R., Gounon,P., Ohayon,H. and Cossart,P. (1993) *J. Cell Sci.*, **105**, 699–710.

Laemmli,U.K. (1970) *Nature*, **227**, 680–685.

Leevers,S.J., Paterson,H.F. and Marshall,C.J. (1994) *Nature*, **369**, 411–414.

Machesky,L.M. and Pollard,T.D. (1993) *Trends Cell Biol.*, **3**, 381–385.

Matthias,P.D., Bernard,H.U., Scott,A., Brady,G., Hashimoto-Gotoh,T. and Schütz,G. (1983) *EMBO J.*, **2**, 1487–1492.

Miller,J. and Germain,R.N. (1986) *J. Exp. Med.*, **164**, 1478–1489.

Okabe,S. and Hirokawa,N. (1989) *J. Cell Biol.*, **109**, 1581–1595.

Pistor,S., Chakraborty,T., Niebuhr,K., Domann,E. and Wehland,J. (1994) *EMBO J.*, **13**, 758–763.

Reggio,H., Webster,P. and Louvard,D. (1983) *Methods Enzymol.*, **98**, 379–396.

Sambrook,J., Fritsch,E.F. and Maniatis,T. (1989) *Molecular Cloning. A Laboratory Manual*. 2nd edn. Cold Spring Harbor Laboratory Press, Cold Spring Harbor, NY.

Sanders,M.C. and Wang,Y.-L. (1990) *J. Cell Biol.*, **110**, 359–365.

Schwartz,D. (ed.) (1963) *Méthodes Statistiques ò-l'Usage des Médecins et des Biologistes*. 3rd edn. Flammarion Médecine Sciences, 296 pp.

Shariff,A. and Luna,E.J. (1990) *J. Cell Biol.*, **110**, 681–692.

Small,J.V., Isenberg,G. and Celis,J.E. (1978) *Nature*, **272**, 638–639.

Sohn,R.H. and Goldschmidt-Clermont,P.J. (1994) *BioEssays*, **16**, 465–472.

Southwick,F.S. and Purich,D.L. (1994) *Proc. Natl Acad. Sci. USA*, **91**, 5168–5172.

Stokoe,D., Macdonald,S.G., Cadwallader,K., Symons,M. and Hancock,J.F. (1994) *Science*, **264**, 1463–1467.

Symons,M.H. and Mitchison,T.J. (1991) *J. Cell Biol.*, **114**, 503–513.

Temm-Grove,C.J., Jockusch,B.M., Rohde,M., Niebuhr,K., Chakraborty,T. and Wehland,J. (1994) *J. Cell Sci.*, **107**, 2951–2960.

Theriot,J.A. and Mitchison,T.J. (1991) *Nature*, **352**, 126–131.

Theriot,J.A., Mitchison,T.J., Tilney,L.G. and Portnoy,D.A. (1992) *Nature*, **357**, 257–260.

Theriot,J.A., Rosenblatt,J., Portnoy,D.A., Goldschmidt-Clermont,P.J. and Mitchison,T.J. (1994) *Cell*, **76**, 505–517.

Tilney,L.G. and Portnoy,D.A. (1989) *J. Cell Biol.*, **109**, 1597–1608.

Tilney,L.G., Connelly,P.S. and Portnoy,D.A. (1990) *J. Cell Biol.*, **111**, 2979–2988.

Tilney,L.G., DeRosier,D.J. and Tilney,M.S. (1992a) *J. Cell Biol.*, **118**, 71–81.

Tilney,L.G., DeRosier,D.J., Weber,A. and Tilney,M.S. (1992b) *J. Cell Biol.*, **118**, 83–93.

Tranter,M.,P., Sugrue,S.P. and Schwartz,M.A. (1989) *J. Cell Biol.*, **109**, 2833–2840.

Vazquez-Boland,J.-A., Kocks,C., Dramsi,S., Ohayon,H., Geoffroy,C., Mengaud,J. and Cossart,P. (1992) *Infect. Immun.*, **60**, 219–230.

Wang,Y.-L. (1985) *J. Cell Biol.*, **101**, 597–602.

Wuestehube,L.J. and Luna,E.J. (1987) *J. Cell Biol.*, **105**, 1741–1751.

Received on February 24, 1995; revised on March 30, 1995